Substrate Determinants of the Course of Tartrate Dehydrogenase-Catalyzed Reactions†

Peter Serfozo and Peter A. Tipton*

Department of Biochemistry, University of Missouri-Columbia, Columbia, Missouri 65211

Received December 19, 1994; Revised Manuscript Received March 27, 1995®

ABSTRACT: The substrate specificity of tartrate dehydrogenase has been probed using a series of alternative substrates to identify the molecular interactions which determine whether a particular substrate undergoes enzyme-catalyzed decarboxylation or not. A series of 3-substituted malate analogs, in which F, Cl, Br, I, SH, or NH_2 substituents were placed at the 3*R*- or 3*S*-position, was prepared, and the product resulting from the action of tartrate dehydrogenase on each compound was identified. All of the halomalates and both diastereomers of aminomalate underwent oxidative decarboxylation; both diastereomers of 3-thiomalate underwent net nonoxidative decarboxylation. The results were interpreted in terms of a model in which decarboxylation is conformationally controlled. The data are not consistent with a model which suggests that substrates assume the conformation that is necessary to avoid steric crowding between the enzyme and the substituent at the 3-position of the substrate. These data are consistent with a model in which the course of the reaction with (+)-tartrate and *meso*-tartrate is dictated by the coordination of the substrate hydroxyls to the active site Mn^{2+}. However, the observed reactivities of the 3-methyltartrate diastereomers are not consistent with this model, either: (2*R*,3*R*)-3-methyltartrate undergoes oxidative decarboxylation, and (2*R*,3*S*)-3-methyltartrate undergoes simple oxidation. These results suggest that for these compounds the conformation is dictated by the positioning of the hydrophobic substituent in a specific binding pocket. In fact, the similarity in the K_m values for all the (2*R*,3*S*)-3-substituted substrates suggest that they share a common binding mode; the K_m's for the (2*R*,3*R*)-3-substituted substrates are much higher and vary widely, suggesting that they bind in an alternative mode.

The first step in the metabolism of (+)-tartrate is its NAD-dependent oxidation to the β-keto acid 3*R*-oxaloglycolate, which is catalyzed by tartrate dehydrogenase. TDH[1] does not catalyze the decarboxylation of 3*R*-oxaloglycolate; however, *meso*-tartrate[2] and D-malate are also substrates for TDH and undergo enzyme-catalyzed decarboxylations (Scheme 1). In the case of D-malate, the overall reaction is an oxidative decarboxylation to yield pyruvate, CO_2, and NADH; *meso*-tartrate is converted to glycerate and CO_2 via a net nonoxidative decarboxylation (Tipton & Peisach, 1990). TDH exhibits substantial homology with β-isopropylmalate dehydrogenase (Tipton & Beecher, 1994), which catalyzes the oxidative decarboxylation of β-isopropylmalate. We have proposed that the multiple catalytic activities of TDH stem from a branched pathway, so that the timing of the release of enzyme-bound species determines the nature of the product (Tipton & Peisach, 1990). To elaborate on this

Scheme 1

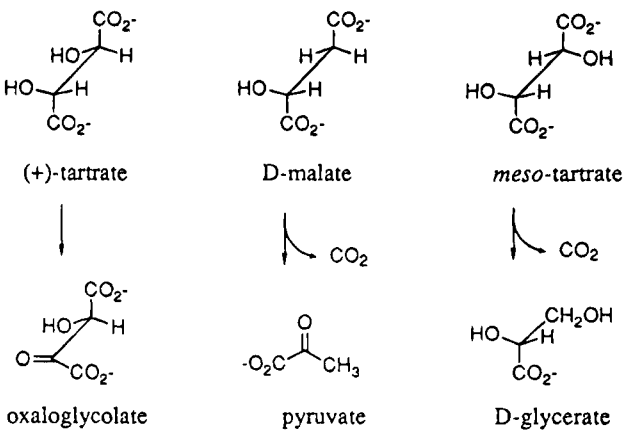

model, it is necessary to explain why the enzyme treats equivalent species, i.e., the β-keto acids formed from each of the three substrates, differently. This information should help realize the goal of providing a quantitative description of the differences between the pathways and may provide insight into the mechanisms by which enzymes can acquire novel catalytic activities through evolution.

Perhaps the simplest hypothesis which explains the different fates of the β-keto acids formed along the reaction pathway is that they assume different conformations at the active site. The importance of substrate conformation as a mechanism to manipulate substrate reactivity in enzymatic reactions has long been recognized. A classic example was provided by Dunathan (1966), who pointed out that the multiplicity of reactions occurring from pyridoxal−Schiff

† Supported by NIH Grant GM46836. The NMR spectrometer used in these studies was obtained with funds from the National Science Foundation, Grant 9221835.

* Address correspondence to this author. Telephone: (314) 882-7968. Fax: (314) 884-4812. E-mail: muccgw.bctipton@ssgate.missouri.edu.

® Abstract published in *Advance ACS Abstracts,* May 15, 1995.

[1] Abbreviations: TDH, tartrate dehydrogenase; LDH, lactate dehydrogenase; ICDH, isocitrate dehydrogenase; IPMDH, β-isopropylmalate dehydrogenase; MDH, malate dehydrogenase; PEP carboxylase, phosphoenolpyruvate carboxylase; PEP; phosphoenolpyruvate; HEPES, *N*-(2-hydroxyethyl)piperazine-*N*′-2-ethanesulfonic acid; DTT, dithiothreitol; HPLC, high-performance liquid chromatography.

[2] (+)-Tartrate is (2*R*,3*R*)-tartrate; *meso*-tartrate is (2*R*,3*S*)-tartrate; D-malate is 2*R*-malate; β-isopropylmalate is (2*R*,3*S*)-3-isopropylmalate. The species we refer to as 3-methyltartrate is 2,3-dihydroxy-3-methylsuccinic acid. In all TDH-catalyzed reactions, the hydroxyl group at the 2-position is oxidized.

0006-2960/95/0434-7517$09.00/0

base adducts could be rationalized by recognizing that the sissile bond would be the one orthogonal to the planar intermediate π system. It has also been noted that production of methylglyoxal from the enediolate phosphate intermediate in the triose phosphate isomerase reaction is minimized by controlling the conformation of the intermediate, so that proton abstraction is favored over phosphate release (Alber et al., 1981). The stereoelectronic basis of enzyme specificity, which is implicit in the idea of conformational control, has been reviewed (Benner, 1988).

Conformational control also plays a role in the decarboxylation of β-keto acids. Overlap between the carbonyl π bond and the σ^* orbital at the sp^3-hybridized carbon to which the leaving carboxyl group is attached occurs when the carboxyl group is orthogonal to the plane defined by the carbonyl group (Pollack, 1978). The constraint this places on substrates of decarboxylases was illustrated by the demonstration that only one of the enantiomers of the conformationally restricted species cyclohexanone 2-carboxylate was a substrate for acetoacetate decarboxylase (Benner & Morton, 1981).

Conformational control could be employed by TDH to prevent the decarboxylation of oxaloglycolate produced from (+)-tartrate. It seems to be a sound assumption that decarboxylation of the intermediate β-keto acids will occur only when they are in the proper conformation; thus, the issue to be addressed is how the conformation of the substrate is determined. By preparing 3-substituted malate analogs which differed with respect to the size, electronegativity, hydrogen-bonding capability, and metal-coordination propensity at the 3-position, we sought to identify the enzyme–substrate interactions which dictate the substrate conformation.

MATERIALS AND METHODS

The gene encoding TDH has been cloned into the pET-3a expression vector (Novagen); TDH was purified from *Escherichia coli* cells harboring this plasmid as described previously (Tipton & Beecher, 1994). Lactate dehydrogenase and phosphoenolpyruvate carboxylase were purchased from Boehringer Mannheim; yeast alcohol dehydrogenase and malate dehydrogenase were purchased from Sigma. Other common biochemicals were from Sigma.

Syntheses. The details of the syntheses are provided in the Supplementary Material. The malate analogs were synthesized from (+)-tartrate-2,3-cyclic sulfate and *meso*-tartrate-2,3-cyclic sulfate, which were prepared from (+)-tartrate and *meso*-tartrate diethyl esters, respectively (Gao & Sharpless, 1988). Starting materials were purchased from Aldrich Chemical. Briefly, (2*R*, 3*S*)-3-substituted malates were prepared by opening the (2*R*, 3*R*)-tartrate diethyl ester-2,3-cyclic sulfate with the appropriate nucleophile. To prepare the halomalates, the nucleophiles were tetraethylammonium halides. 3-Thiomalate was derived from the product obtained by nucleophilic addition of thiosulfate to the tartrate cyclic sulfate; 3-aminomalate was derived from azidomalate, prepared by addition of azide to the tartrate cyclic sulfate. The (2*R*, 3*R*)-3-substituted compounds were prepared in an analogous fashion from the *meso*-tartrate diethyl ester-2,3-cyclic sulfate. This route resulted in a mixture of the (2*R*, 3*R*)- and (2*S*, 3*S*)-3-substituted compounds, which was deemed satisfactory for these studies, since (2*S*)-2-hydroxyacids appear not to bind to TDH. The 3-methyltartrates[2] were synthesized by sodium tungstate-catalyzed dihydroxylation of citraconic acid and mesaconic acid (Church & Blumberg, 1951).

^{1}H NMR Analysis of the Catalytic Reactions. For those substrates whose turnover generated NADH, the reactions were monitored using ^{1}H NMR. Each reaction was carried out in a 5 mm NMR tube; the reaction solutions were prepared in D_2O and contained 20−40 mM malate analog, 0.4 mM NAD^+, 0.15 mM β-mercaptoethanol, 20 mM $MgSO_4$, and 3-(trimethylsilyl)propionic-*2,2,3,3-d*$_4$ acid as an internal chemical shift reference, in 100 mM potassium phosphate, pH 8.0. Although Mn^{2+} is used in routine assays of TDH, Mg^{2+} is able to replace it with only a 2-fold reduction in V_{max} (Tipton & Peisach, 1990). To facilitate the analysis of the outcome of the catalytic reaction, described below, and to recycle the NAD^+, 100−600 units of lactate dehydrogenase was present in each sample. For analysis of the aminomalates, lactate dehydrogenase was omitted, and the NADH was recycled by including yeast alcohol dehydrogenase and acetone in the assay solutions. Spectra were obtained at 250 MHz with a Bruker ARX-250. For each substrate analog, a spectrum of the assay solution without TDH was obtained, and the reaction was initiated by the addition of 0.2−0.5 units of TDH. Spectra were obtained periodically until the reaction was completed.

HPLC Analysis of the Thiomalate Reaction Products. The products of the TDH-catalyzed reactions of (2*R*,3*S*)-3-thiomalate and (2*R*,3*R*)-3-thiomalate were identified by HPLC. TDH was incubated with each diastereomer of 3-thiomalate, 0.4 mM $Mn(OAc)_2$, and 1.5 mM NAD^+ in a volume of 0.5 mL, and the reaction was quenched after 30, 60, and 90 s, by the addition of 50 μL of $CHCl_3$, followed by vigorous vortexing. To each sample was added 10 μL of 20 mM 5,5′-dithiobis(2-nitrobenzoic acid) dissolved in ethanol to convert the thiol compounds present in the sample to the corresponding nitrobenzoic acid mixed disulfides. A 100 μL aliquot of the derivatized reaction mixture was applied to a Spherisorb ODS-2 C-18 reverse-phase column (250 × 4.6 mm) equilibrated in buffer consisting of 5% acetonitrile in 10 mM H_3PO_4 and 100 mM NaCl, pH 2.2. The column was eluted at a flow rate of 1.0 mL/min with a program composed of a 40 min gradient from the equilibration buffer to buffer containing 40% acetonitrile in 10 mM H_3PO_4 and 100 mM NaCl, pH 3.51, followed by a 15 min wash in the second buffer. The derivatized species were detected by their absorbance at 342 nm. The product of the enzymatic reaction was identified by comparison of its retention time with an authentic sample of thioglycerate (2-hydroxy-3-mercaptopropionate).

Identification of Aminomalate and 3-Methyltartrate Reaction Products. The products of the aminomalate reactions were not amenable to analysis by NMR or HPLC for reasons discussed below. Also, it could not be determined from NMR or HPLC analyses whether the methyltartrate diastereomers underwent TDH-catalyzed oxidative decarboxylation or simple oxidation. Therefore, the nature of each catalytic reaction was inferred from kinetics experiments in which the CO_2 produced in the TDH-dependent reaction was trapped enzymatically, using a coupled assay with phosphoenolpyruvate carboxylase and malate dehydrogenase. Each sample contained 0.5 mM NAD^+, 1.2 mM substrate, 2.5 mM PEP, 20 mM $MgSO_4$, 1 mM DTT, and 15 units of MDH in

a stoppered cuvette. PEP carboxylase (0.25 unit) and sufficient NADH (0.7−0.8 mM) were added to remove contaminating CO_2, and the reaction was initiated by the addition of TDH (0.1 units). Neither 3-methyltartrate nor 3-aminomalate was a substrate for MDH or inhibited PEP carboxylase. When TDH-catalyzed decarboxylation occurred, NADH and CO_2 production were stoichiometric, and each product was trapped by the coupling enzymes: CO_2 by PEP carboxylase to generate OAA, and NADH by malate dehydrogenase which catalyzed the reduction of the OAA. Thus, when TDH catalyzed the oxidative decarboxylation of its substrate, no net NADH formation was observed. Conversely, oxidation of the substrate without decarboxylation led to net NADH production.

Steady-State Kinetics. Oxidative reactions were monitored by measuring the rate of formation of NADH (λ_{max}, 340 nm; ϵ, 6220 M^{-1} cm^{-1}). Reactions were carried out in 1 cm path length quartz cuvettes thermostated at 25 °C. Data were obtained with a Beckman DU monochromater interfaced to a personal computer for data acquisition and analysis and with a Hewlett-Packard 8452A diode array spectrophotometer. The activity of TDH was determined on a daily basis by measuring the velocity of a reaction under standard conditions, which were 10 mM (+)-tartrate, 1.5 mM NAD^+, 0.4 mM $Mn(OAc)_2$, and 1 mM DTT in 100 mM K^+ HEPES at pH 8.0. Data collected each day were normalized using the velocity obtained in the standard assay in order to facilitate the comparison of data obtained at different times. The reactions with the alternative substrates were performed in 100 mM K^+ HEPES, pH 8.0, containing 1.5 mM NAD^+, 0.4 mM $Mn(OAc)_2$, and 1 mM DTT. Initial velocity data were fitted to the equation $v = V_{max}A/(K_m + A)$, in which A is the variable substrate concentration, by nonlinear least-squares methods.

RESULTS

The following compounds were prepared from (+)-tartrate diethyl ester 2,3-cyclic sulfate: (2*R*, 3*S*)-3-fluoromalate, (2*R*, 3*S*)-3-chloromalate, (2*R*, 3*S*)-3-bromomalate, (2*R*, 3*S*)-3-iodomalate, (2*R*, 3*S*)-3-thiomalate, and (2*R*, 3*S*)-3-aminomalate. The corresponding (2*R*, 3*R*) compounds were prepared [as mixtures with the (2*S*, 3*S*) compounds] from *meso*-tartrate diethyl ester 2,3-cyclic sulfate.

Table 1 lists the type of reaction TDH catalyzed with each substrate and the ^1H NMR characteristics of the product of each experiment. The kinetic parameters for all those substrates which underwent oxidative reactions are listed in Table 2.

Because oxidation of each halogenated substrate to the corresponding β-keto acid would generate a relatively unstable compound which would be subject to nonenzymatic decarboxylation under the experimental conditions, some care was taken to determine whether decarboxylated products arose nonenzymatically or from the action of TDH. This distinction was made with the following experiment, which is diagrammed in Scheme 2. The catalytic reaction was performed in D_2O and monitored by ^1H NMR. Decarboxylation of the β-keto acid generates the corresponding enolate as the immediate product; ketonization of the enolate incorporates a deuteron from the solvent into the product keto acid. If this occurs at the active site of TDH, it should occur stereospecifically. If, however, the enolate ketonizes in solution, as a result of nonenzymatic decarboxylation, deuteron incorporation will not be stereospecific. Reduction of the keto acid to the corresponding 2-hydroxy acid generates a chiral center and renders the methylene protons at C-3 diastereotopic and distinguishable by ^1H NMR (Figure 1A). Thus, ^1H NMR analysis reveals whether solvent deuterium incorporation occurred stereospecifically, indicative of enzyme-catalyzed decarboxylation, or nonstereospecifically, indicative of nonenzymatic decarboxylation. For the halomalate substrates of TDH, stereospecific reduction of the product keto acids was achieved using lactate dehydrogenase, which also recycled the NADH which was produced stoichiometrically with the oxidation of the halomalate substrate. Reduction of the keto acids also prevented the deuterium incorporated into the methylene carbon from exchanging with solvent; furthermore, since the NAD^+ was recycled by this scheme, it was possible to include it at concentrations 50−100-fold below the concentration of the halomalate substrate and so was not visible in the ^1H NMR spectrum. The time course for the TDH-catalyzed turnover of (2*R*,3*S*)-3-bromomalate is shown in Figure 1B. One methylene proton signal appears at 3.75 ppm as a broadened

Table 1: Products of the TDH Reactions

substrate	peak positions (ppm)	J_{HH} (Hz)	reaction
(2*R*,3*S*)-3-fluoromalate	4.67; 4.28	4.5	oxidative decarb
(2*R*,3*S*)-3-chloromalate	4.34; 3.86	4.6	oxidative decarb
(2*R*,3*S*)-3-bromomalate	4.34; 3.73	4.6	oxidative decarb
(2*R*,3*S*)-3-iodomalate	4.09; 3.50	3.6	oxidative decarb
(2*R*,3*S*)-3-thiomalate	n.d.[b]	n.d.	net non-ox. decarb
(2*R*,3*S*)-3-aminomalate	no observable product		oxidative decarb
(2*R*,3*R*)-3-fluoromalate	4.56[a]; 4.28	n.d.[c]	oxidative decarb
(2*R*,3*R*)-3-chloromalate	4.36; 3.85	n.d.[c]	oxidative decarb
(2*R*,3*R*)-3-bromomalate	4.34; 3.72	n.d.[c]	oxidative decarb
(2*R*,3*R*)-3-iodomalate	4.10; 3.80[d]	n.d.[c]	oxidative decarb
(2*R*,3*R*)-3-thiomalate	n.d.	n.d.	net non-ox decarb
(2*R*,3*R*)-3-aminomalate	no observable product		oxidative decarb
(2*R*,3*R*)-3-methyltartarte	n.d.	n.d.	oxidative decarb
(2*R*,3*S*)-3-methyltartrate	n.d.	n.d.	oxidation

[a] This signal is the upfield half of the doublet arising from the C2 proton, which is strongly coupled to F; the downfield signal is under the HDO peak. [b] n.d., not determined. [c] These spectra deviated from first order appearance, and coupling constants were not extracted from the data. [d] This spectrum appeared to arise from a mixture of iodolactate and glycerate formed from the hydrolysis of iodolactate.

Table 2: Kinetic Parameters for Substrates of TDH[a]

compound	V_{max} (relative)	V/K (mM^{-1})	K_m (mM)
(+)-tartrate[b]	1	1.0	1.0
(2*R*,3*R*)-3-fluoromalate	0.23 ± 0.01	0.35 ± 0.04	0.67 ± 0.11
(2*R*,3*R*)-3-chloromalate	1.48 ± 0.01	5.49 ± 0.14	0.27 ± 0.09
(2*R*,3*R*)-3-bromomalate	0.82 ± 0.07	3.8 ± 0.6	0.22 ± 0.05
(2*R*,3*R*)-3-iodomalate	14.6 ± 0.9	600 ± 120	0.024 ± 0.006
(2*R*,3*R*)-3-aminomalate	0.48 ± 0.01	0.83 ± 0.05	0.58 ± 0.05
(2*R*,3*R*)-3-methyltartrate	1.85 ± 0.07	31 ± 4	0.060 ● 0.009
D-malate[b]	40	800	0.05
meso-tartrate	1.24 ± 0.07	21 ± 4	0.06 ± 0.01
(2*R*,3*S*)-3-fluoromalate	1.80 ± 0.02	96 ± 4	0.019 ± 0.001
(2*R*,3*S*)-3-chloromalate	2.10 ± 0.06	160 ± 20	0.012 ± 0.002
(2*R*,3*S*)-3-bromomalate	6.20 ± 0.08	550 ± 40	0.011 ± 0.008
(2*R*,3*S*)-3-iodomalate	19 ± 1	720 ± 90	0.027 ± 0.005
(2*R*,3*S*)-3-aminomalate	0.57 ± 0.02	22 ± 2	0.026 ± 0.003
(2*R*,3*S*)-3-methyltartrate	2.49 ± 0.06	35 ± 3	0.070 ± 0.008

[a] Velocities are defined relative to the velocity of the (+)-tartrate reaction under standard conditions, as described in the Methods section. V_{max} for this reaction is 0.71 μmol min^{-1} mg^{-1} (Tipton and Peisach (1990). [b] Data are taken from Tipton and Peisach (1990).

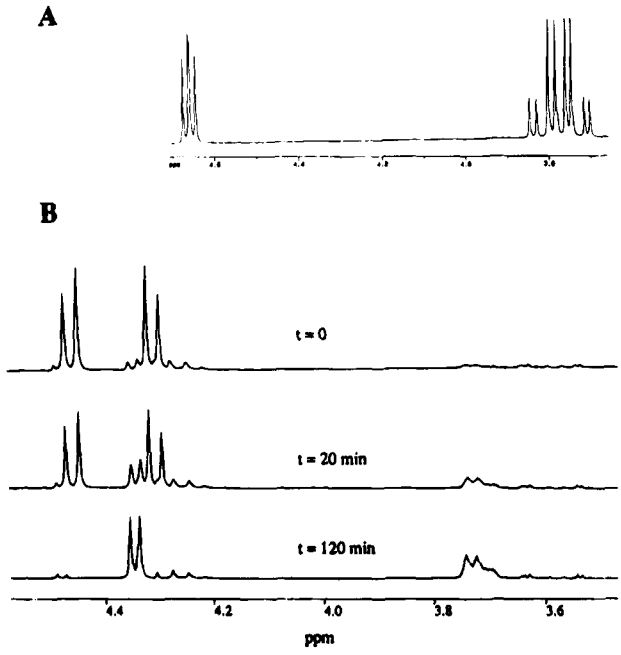

FIGURE 1: (A) ^{1}H NMR spectrum of authentic bromolactate at pD 2, obtained in D_2O. (B) Time course of TDH-catalyzed turnover of (2*R*,3*S*)-3-bromomalate in D_2O. Experimental conditions are given in the text.

doublet due to geminal coupling to deuterium. The C-2 proton appears at 4.35 ppm as a doublet, indicating that it is coupled to a single proton. It is apparent that incorporation of solvent deuterium is stereospecific and thus indicates that the substrate was oxidatively decarboxylated by TDH.

The spectrum of chlorolactate resulting from the actions of TDH and lactate dehydrogenase on (2*R*,3*R*)-3-chloromalate is shown in Figure 2. Similar spectra were obtained for all the (2*R*,3*R*)-3-halomalates. Although the spectra deviate considerably in appearance from simple first-order

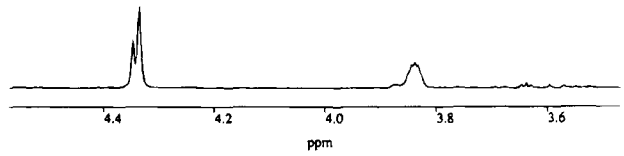

FIGURE 2: ^{1}H NMR spectrum of the product of the TDH-catalyzed turnover of (2*R*,3*R*)-3-chloromalate in D_2O. Experimental conditions are given in the text.

spectra, they are most consistent with the assignment of stereospecifically deuterated halolactates. The possibility that the spectra arose from the superposition of more than one species was excluded by chromatographic purification and characterization of chlorolactate and of bromolactate; each yielded a ^{1}H NMR spectrum identical to that seen in the reaction mixture (data not shown).

The ^{1}H NMR analysis failed for the aminomalates, because the TDH-generated product could not be trapped by lactate dehydrogenase. NMR analysis of the catalytic reactions revealed that no new ^{1}H signals arose as the substrates were oxidized. These results are explicable in view of the fact that the likely products of the reactions would enolize and exchange their protons with the solvent deuterium. However, this could occur with either 3-aminooxalacetate or 3-aminopyruvate. Attempts to analyze the reaction products were further complicated by the fact that the products underwent secondary reactions, suggested by the observation that the solutions turned yellow as the reactions progressed. Attempts to derivatize the aminomalate reaction products with dinitrofluorobenzene also failed, presumably as a result of facile tautomerization and secondary reactions between the products. Therefore, the identity of the products was inferred by trapping the CO_2 resulting from the action of TDH on the aminomalates. The coupled assay system used in these experiments was described above; for both diastereomers of aminomalate, no net NADH production was observed,

Scheme 2

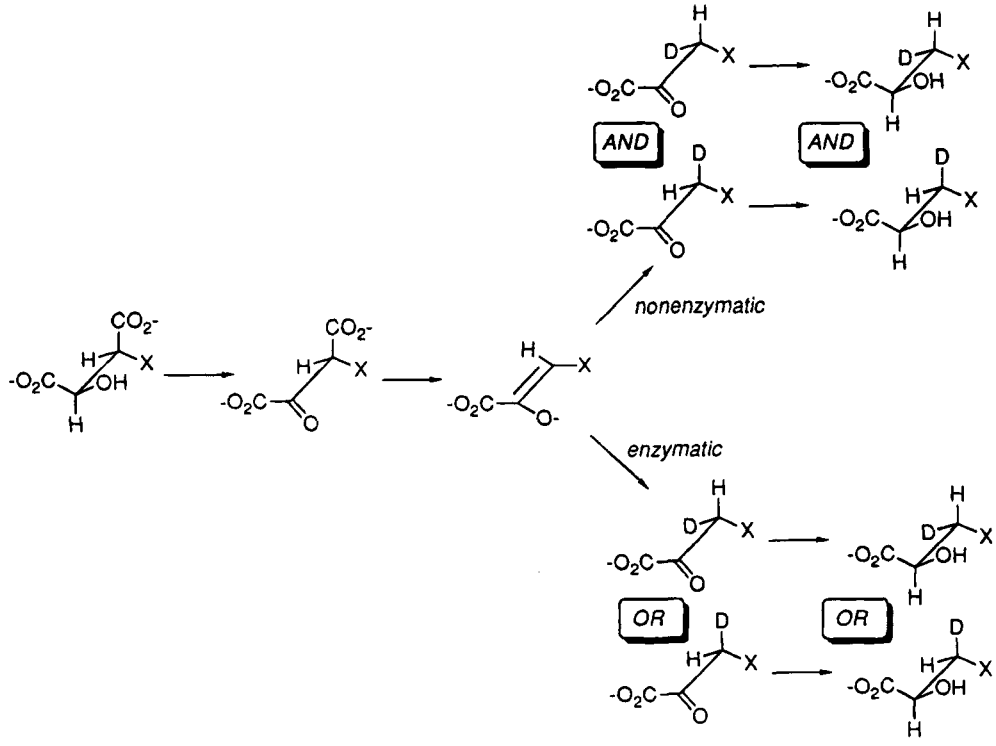

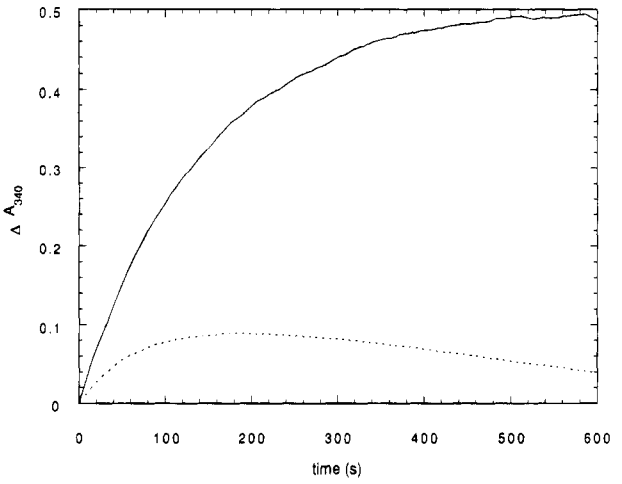

FIGURE 3: Time course for the reactions of (2R,3S)-3-methyltartrate (solid line) and (2R,3R)-3-methyltartrate (dashed line) with TDH, using the PEP carboxylase–MDH coupled assay. Experimental conditions are given in the text.

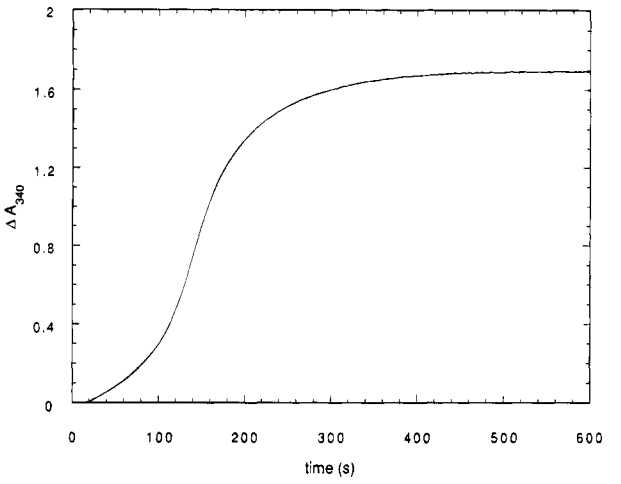

FIGURE 4: Time course for the reaction of a mixture of (2*R*,3*S*)-3-thiomalate and D-malate. The solution contained 20 μM (2*R*,3*S*)-3-thiomalate, 300 μM D-malate, 0.4 mM $Mn(OAc)_2$, 0.6 mM NAD^+, and 1 mM DTT in 100 mM HEPES, pH 8.0.

demonstrating stoichiometric production of NADH and CO_2 from the TDH reaction and suggesting that TDH catalyzed the direct formation of aminopyruvate and CO_2.

When this coupled assay was applied to the 3-methyltartrate reactions, the results shown in Figure 3 were obtained. It is apparent that there is net NADH production when TDH catalyzes the turnover of (2*R*,3*S*)-3-methyltartrate; the cessation of NADH production after 5 min is probably attributable to nonenzymatic decarboxylation of the product β-keto acid. In contrast, it appears the TDH-catalyzed turnover of (2*R*,3*R*)-3-methyltartrate does not yield net NADH production in the coupled assay system. The small burst of NADH observed most likely arises from a lag in the coupled enzyme assay. It is important to note that both experiments were conducted under saturating conditions where the TDH-catalyzed reactions proceeded at approximately the same velocity. The large difference in initial rates observed in Figure 3 does not correspond quantitatively with the 30% difference in V_{max}'s between the two diastereomers of 3-methyltartrate.

Incubation of either diastereomer of 3-thiomalate with TDH did not result in the production of NADH. Preliminary evidence that they were substrates of TDH was obtained by incubating a mixture of 3-thiomalate and D-malate with the enzyme. Initially, no NADH production was observed, but over time NADH was generated at an increasing rate, until the reaction approached completion (Figure 4). This time course arises because the D-malate reaction, which generates NADH, is inhibited by the 3-thiomalate reaction until TDH turns over sufficient 3-thiomalate that D-malate can compete successfully for the enzyme. Similar behavior is observed when the D-malate reaction is conducted in the presence of *meso*-tartrate. The product of that reaction has been identified as D-glycerate, which arises via sequential oxidation, decarboxylation, and reduction of the substrate (Tipton & Peisach, 1990). Thus, the overall reaction is NAD-dependent net nonoxidative decarboxylation of *meso*-tartrate and is spectroscopically silent at 340 nm. An analogous sequence of events with 3-thiomalate would yield thioglycerate as the product. Indeed, thioglycerate was identified as the product of the reactions of both diastereomers of 3-thiomalate, on the basis of its HPLC chromatographic behavior. The derivatized products of the thiomalate reactions eluted after 30.6 min, as did an authentic sample of derivatized thioglycerate. Derivatized thiomalate eluted at 26.4 min.

DISCUSSION

One of the more curious aspects of TDH is the multiplicity of catalytic activities it displays. Although three of its substrates, (+)-tartrate, D-malate, and *meso*-tartrate, differ only with respect to the presence or absence of a hydroxyl group at the 3*R* or 3*S* position, each undergoes a different chemical reaction. This demonstrates that relatively subtle aspects of the enzyme–substrate complex can influence the catalytic reaction profoundly. It is intriguing to speculate on the role that these interactions may have played in the evolution of TDH.

A puzzling feature of TDH is the sluggishness with which it catalyzes the oxidation of (+)-tartrate, the presumptive "natural substrate" of the enzyme, which is functionally defined by the fact that the host bacteria were isolated by virtue of their ability to grow on tartrate media (Kohn & Jakoby, 1968) and the fact that the enzyme is produced only when the host bacteria are grown on media containing (+)-tartrate as the sole carbon source. We have suggested that TDH is an evolutionarily young enzyme which arose when the bacteria recruited a preexisting enzyme capable of catalyzing the necessary reaction with (+)-tartrate, and that the poor catalytic properties stem from the fact that the enzyme has not yet evolved to its maximal potential as a catalyst for the new reaction. Sequence analysis suggests that the progenitor enzyme is β-isopropylmalate dehydrogenase (Tipton & Beecher, 1994), which catalyzes the oxidative decarboxylation of isopropylmalate in the leucine biosynthetic pathway. Recruitment of preexisting enzymes on the basis of their abilities to catalyze a required chemical transformation, not their substrate binding abilities, per se, has been proposed to be a general mechanism for enzyme evolution (Petsko et al., 1993), and TDH may be well-suited for the study of how a new enzyme evolves from an earlier one. In particular, it is important to define how the enzyme utilizes the intrinsic chemical reactivity of the substrate when appropriate and minimizes unwanted reactions when necessary.

Scheme 3

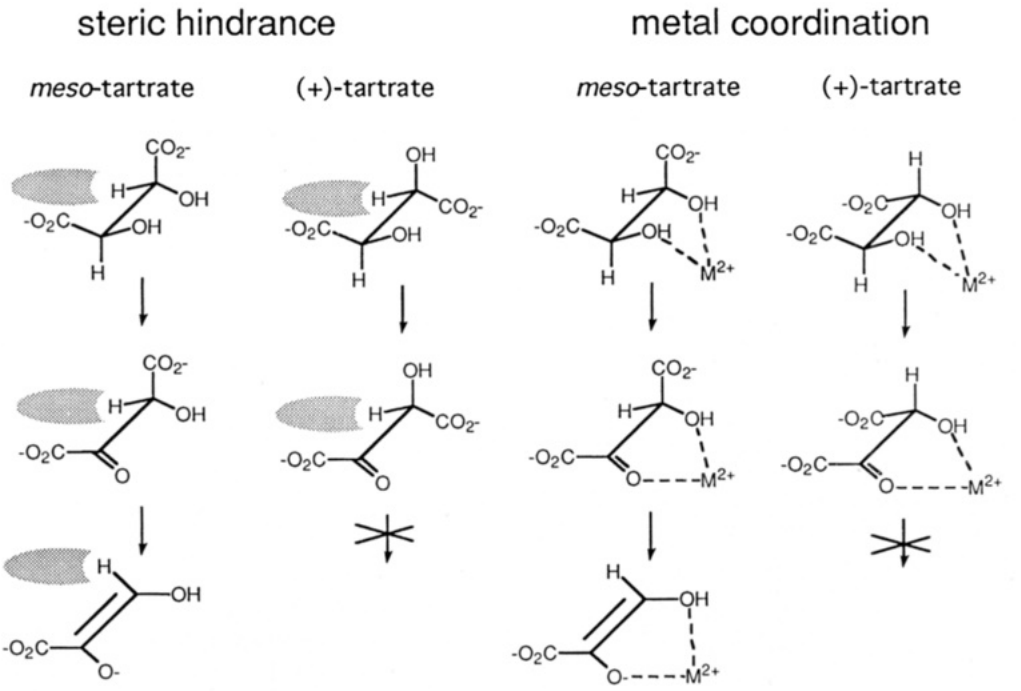

TDH catalyzes the formation of 3*R*-oxaloglycolate from (+)-tartrate and D-glycerate from *meso*-tartrate. It is proposed that D-glycerate arises from the oxidation of *meso*-tartrate to 3*S*-oxaloglycolate, followed by decarboxylation, and NADH-dependent reduction of the resulting hydroxypyruvate (Tipton & Peisach, 1990). One question raised by this presumptive sequence of events is why the enzyme catalyzes the decarboxylation of 3*S*-oxaloglycolate and not 3*R*-oxaloglycolate. Presumably the answer lies in the different conformations assumed by the two substrates at the active site of TDH; i.e., 3*S*-oxaloglycolate assumes a conformation appropriate for decarboxylation, with the leaving carboxyl group orthogonal to the plane defined by the C-2 carbonyl, and 3*R*-oxaloglycolate binds in a conformation from which decarboxylation is disfavored. However, this explanation simply raises another question: How does the enzyme control the conformation of the substrate?

Two possibilities are readily envisioned (Scheme 3). When (+)-tartrate and *meso*-tartrate are arranged in conformations consistent with their observed reactivities, two features are notable. The first is that both substrates have the proton attached to C-3 occupying the same position in space. This suggests that the enzyme active site may be constructed such that a larger substituent cannot be tolerated at that position, and so the substrates rotate about the C-2, C-3 bond to place the hydrogen there. A second possibility is that the active site Mn^{2+} plays a role in determining the substrate conformation. As drawn in Scheme 3, both (+)-tartrate and *meso*-tartrate can have their hydroxyl groups arranged for facile bidentate coordination to Mn^{2+}.

The reactivities of a series of substrate analogs were examined to evaluate the merits of these models. The halomalates differ in electronegativity and, more importantly, in the size of the substituent at the 3-position. The thiomalates and aminomalates are potentially capable of hydrogen-bonding interactions like the tartrate hydroxyl groups but differ from the tartrates in their metal-coordinating propensities.

Significantly, all of the halomalates underwent enzyme-catalyzed oxidative decarboxylation, regardless of whether the halogen occupied the 3*S*-position or the 3*R*-position. With the (2*R*,3*R*)-3-substituted halomalates, the halogen is placed in the position in space occupied by the C-3 proton in (+)-tartrate and *meso*-tartrate in the steric hindrance model shown in Scheme 3; the substrates examined in this study cover a wide enough range in size that if steric constraints were acting at the active site, some of the halomalates should not have been accommodated. In the crystal structure of sodium D-tartrate, the distances between the hydroxyl oxygens and C2 and C3 are 1.414 and 1.420 Å; the distances between the hydroxyl oxygens and the hydrogens attached to them are 0.89 and 0.77 Å (Ambady & Kartha, 1968). 3*R*-3-Iodomalate presumably has a typical C−I bond length of around 2.1 Å (March, 1985); thus, it is difficult to imagine that the active site would accommodate an iodo substituent and not a hydroxyl group, on the basis of size alone. Therefore, it appears unlikely that steric interactions between the substrate and the enzyme play a defining role in determining the conformation of the substrate.

The data obtained with the substituted malate analogs are more consistent with the metal coordination model shown in Scheme 3. In this model, it is the specific interactions between Mn^{2+} and the tartrate vicinal hydroxyl goups which determine the outcome of the reaction. As a further test of this hypothesis, 3-methyltartrate diastereomers were prepared. However, (2*R*,3*R*)-3-methyltartrate, which is a (+)-tartrate analog with regard to the disposition of its hydroxyl group, underwent oxidative decarboxylation. The other diastereomer, (2*R*,3*S*)-3-methyltartrate, which is a *meso*-tartrate analog, underwent simple oxidation. These results are consistent with the substrates binding in the orientations shown in Scheme 4, in which the methyl group determines the conformation. Such a result is not surprising, considering the homology between TDH and IPMDH. It appears that the methyl groups of the 3-methyltartrate diastereomers are binding in the still-extant pocket in which the isopropyl group

Scheme 4

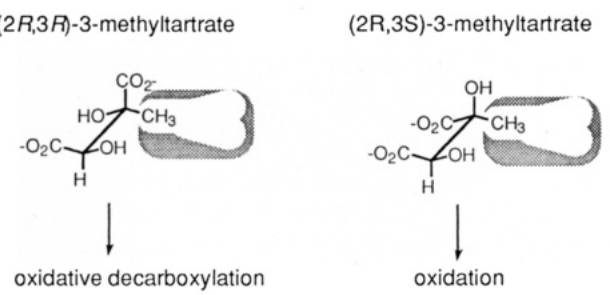

of isopropylmalate binds in IPMDH. [Because of the convention for determining priorities of the substituents at C3 of the substrates in order to assign the R,S configuration, (2*R*,3*R*)-3-methyltartrate has its methyl group in the same place that (2*R*,3*S*)-3-isopropylmalate has its isopropyl group.]

In fact, examination of Table 2 reveals that all the (2*R*,3*S*)-3-substituted substrates have remarkably similar K_m's, suggesting that there is wide latitude for accommodation of 3*S*-substituents. Note that the substrate for IPMDH is (2*R*,3*S*)-3-isopropylmalate. In fact, isopropylmalate is a substrate for TDH with a K_m of 14 μM (Tipton & Beecher, 1994). The K_m's for the (2*R*,3*R*)-3-substituted substrates are higher, and vary widely, suggesting that 3*R*-substituents are not accommodated as easily at the TDH active site. It remains to be determined whether this factor is responsible for the decreased rates of reactions observed with (2*R*,3*R*)-3-substituted species.

Thus it appears that there are at least two binding modes available to substrates at the TDH active site, one reminiscent of the isopropylmalate binding mode, and the one used by (2*R*,3*R*)-3-substituted species, whose defining interactions remain unidentified. It may be that (+)-tartrate binds via coordination to Mn^{2+} as shown in Scheme 3.[3] It should be noted that bidentate coordination of the hydroxyl groups would be a novel coordination scheme in decarboxylating dehydrogenases, although such an arrangement would still allow stabilization of the enolate intermediate generated during the reaction. A coordination scheme analogous to that observed in isocitrate dehydrogenase would place the Mn^{2+} between the C-1 carboxyl and the C-2 hydroxyl (Hurley et al., 1991). This model is consistent with the observation that both diastereomers of 3-thiomalate and 3-aminomalate are decarboxylated by the enzyme: since coordination between the hard acid Mn^{2+} and the softer thiol and amino ligands would not be particularly favorable, coordination likely occurs between the C-1 and C-2 positions, and the C-2, C-3 bond could rotate to allow decarboxylation.

The data in Table 2 demonstrate that the facility with which the substrate is oxidatively decarboxylated increases as the electronegativity of the substituent decreases, as would be expected. These data demonstrate the hydride transfer is at least partially rate-limiting in these transformations. In contrast, hydride transfer is not very rate-limiting in the oxidative decarboxylation of D-malate (Tipton, 1993). A closer examination of these data will be possible when the degree to which hydride transfer is rate-limiting is more precisely known.

An interesting issue is whether abrogation of the decarboxylation reaction in the turnover of (+)-tartrate is a desirable feature of the catalytic reaction. The metabolism of (+)-tartrate in *Pseudomonas* species ultimately generates D-glycerate, either via enzyme-catalyzed reductive decarboxylation of oxaloglycolate, or enzyme-catalyzed conversion of hydroxypyruvate and tartronic semialdehyde, which arise from nonenzymatic breakdown of oxaloglycolate (Kohn & Jakoby, 1968). Therefore, it would be more efficient if TDH turned over (+)-tartrate to D-glycerate directly, as it does with *meso*-tartrate, or catalyzed its oxidative decarboxylation to form hydroxypyruvate. It may be that the failure to catalyze the decarboxylation of 3*R*-oxaloglycolate is an unintended consequence of the enzyme's ability to act on (+)-tartrate, which is trapped in an inappropriate conformation.

A curious feature of the family of reactions catalyzed by TDH is that they suggest that the ionized C-4 carboxyl group does not play a defining role in orienting the substrate, since it is proposed that the different reactions arise from different rotomeric conformations of the substrate. It is noteworthy that TDH requires a monovalent cation for activity, whereas a similar requirement has not been reported for ICDH or IPMDH. Thus, the monovalent cation may serve as a neutralizing charge in the TDH active site which allows the C-4 carboxyl group to bind in different locations, perhaps by occupying different coordination sites on the monovalent cation. The involvement of the monovalent cation may represent a "stop-gap" measure in the evolution of TDH, to achieve charge neutralization until a favorable mutation places a charged residue at the appropriate position in the active site.

This hypothesis can be evaluated using site-directed mutagenesis; another line of inquiry which is planned is random mutagenesis experiments to explore the possibility of increasing the catalytic efficiency of TDH toward (+)-tartrate. Detailed kinetic studies of the alternative substrates which have been identified in this work will also be conducted to determine how the effectiveness of the enzyme changes as the properties of the substrates are changed.

SUPPLEMENTARY MATERIAL AVAILABLE

Synthetic procedures and ^1H NMR spectroscopic data for the compounds used in this study (4 pages). Ordering information is given on any current masthead page.

REFERENCES

Alber, T., Banner, D. W., Bloomer, A. C., Petsko, G. A., Phillips, D., Rivers, P. S., & Wilson, I. A. (1981) *Phil. Trans. R. Soc. London B 293*, 159−171.

Ambady, G. K., & Kartha, G. (1968) *Acta Crystallogr. B24*, 1540−1547.

Benner, S. A. (1988) in *Mechanistic Principles of Enzyme Action* (Liebman, J. F., & Greenberg, A., Eds.) pp 27−74, VCH Publishers, Inc., New York.

Benner, S. A., & Morton, T. H. (1981) *J. Am. Chem. Soc. 103*, 991−993.

Church, J. M., & Blumberg, R. (1951) *Ind. Eng. Chem. 43*, 1780−1786.

Dunathan, H. (1966) *Proc. Natl. Acad. Sci. U.S.A. 55*, 712−716.

[3] Direct coordination of the substrate to the active site Mn^{2+} has not been explicitly demonstrated. However, it is reasonable to propose that direct coordination occurs during turnover, given the nature of the catalytic reactions, and by analogy with isocitrate dehydrogenase. Furthermore, we observe large inverse solvent isotope effects on *V*/*K* with a variety of substrates, which are most reasonably interpreted as arising from coordination of the substrate to Mn^{2+} (M. Dimmic and P. Tipton, unpublished observations).

Gao, Y., & Sharpless, K. B. (1988) *J. Am. Chem. Soc. 110*, 7538−7539.

Hurley, J. H., Dean, A. M., Koshland, D. E., Jr., & Stroud, R. M. (1991) *Biochemistry 30*, 8671−8678.

Imada, K., Sato, M., Tanaka, N., Katsube, Y., Matsuura, Y., & Oshima, T. (1991) *J. Mol. Biol. 222*, 725−738.

Kohn, L. D., & Jakoby, W. B. (1968) *J. Biol. Chem. 243*, 2465−2471.

Kohn, L. D., Packman, P. M., Allen, R. H., & Jakoby, W. B. (1968) *J. Biol. Chem. 243*, 2479−2485.

March, J. (1985) *Advanced Organic Chemistry*, 3rd ed., p 19, John Wiley & Sons, New York.

Petsko, G. A., Kenyon, G. L., Gerlt, J. A., Ringe, D., & Kozarich, J. W. (1993) *Trends Biochem. Sci. 18*, 372−376.

Pollack, R. M. (1978) in *Transition States of Biochemical Processes* (Gandour, R. D., & Schowen, R. L., Eds) pp 467−492, Plenum Press, New York.

Stoddard, B. L., & Koshland, D. E., Jr. (1993) *Biochemistry 32*, 9317−9322.

Stoddard, B. L., Dean, A., & Koshland, D. E., Jr. (1993) *Biochemistry 32*, 9310−9316.

Tipton, P. A. (1993) *Biochemistry 32*, 2822−2827.

Tipton, P. A., & Peisach, J. (1990) *Biochemistry 29*, 1749−1756.

Tipton, P. A., & Beecher, B. S. (1994) *Arch. Biochem. Biophys. 313*, 15−21.

BI942915U